Environmental Research Letters

LETTER

Effects of photochemical oxidation on the mixing state and light absorption of black carbon in the urban atmosphere of China

Qiyuan Wang[1,2], Rujin Huang[1,2,3,7], Zhuzi Zhao[1,2], Junji Cao[1,2,4,7], Haiyan Ni[1], Xuexi Tie[1,2], Chongshu Zhu[1,2], Zhenxing Shen[5], Meng Wang[1], Wenting Dai[1,2], Yongming Han[1,2,4], Ningning Zhang[1,2] and André S H Prévôt[1,6]

[1] Key Laboratory of Aerosol Chemistry and Physics, Institute of Earth Environment, Chinese Academy of Sciences, Xi'an 710061, People's Republic of China
[2] State Key Laboratory of Loess and Quaternary Geology, Institute of Earth Environment, Chinese Academy of Sciences, Xi'an 710061, People's Republic of China
[3] Centre for Atmospheric and Marine Sciences, Xiamen Huaxia University, Xiamen 361024, People's Republic of China
[4] Institute of Global Environmental Change, Xi'an Jiaotong University, Xi'an 710049, People's Republic of China
[5] Department of Environmental Sciences and Engineering, Xi'an Jiaotong University, Xi'an 710049, People's Republic of China
[6] Laboratory of Atmospheric Chemistry, Paul Scherrer Institute (PSI), 5232 Villigen, Switzerland
[7] Author to whom any correspondence should be addressed.

E-mail: cao@loess.llqg.ac.cn and rujin.huang@ieecas.cn

Keywords: black carbon, mixing state, mass absorption cross-section, photochemical oxidation, light absorption

Supplementary material for this article is available online

OPEN ACCESS

RECEIVED
9 September 2016

REVISED
12 February 2017

ACCEPTED FOR PUBLICATION
7 March 2017

PUBLISHED
3 April 2017

Abstract

The relationship between the refractory black carbon (rBC) aerosol mixing state and the atmospheric oxidation capacity was investigated to assess the possible influence of oxidants on the particles' light absorption effects at two large cities in China. The number fraction of thickly-coated rBC particles (F_{rBC}) was positively correlated with a measure of the oxidant concentrations ($OX = O_3 + NO_2$), indicating an enhancement of coated rBC particles under more oxidizing conditions. The slope of a linear regression of F_{rBC} versus OX was 0.58% ppb^{-1} for Beijing and 0.84% ppb^{-1} for Xi'an, and these relationships provide some insights into the evolution of rBC mixing state in relation to atmospheric oxidation processes. The mass absorption cross-section of rBC (MAC_{rBC}) increased with OX during the daytime at Xi'an, at a rate of 0.26 $m^2\ g^{-1}\ ppb^{-1}$, suggesting that more oxidizing conditions lead to internal mixing that enhances the light-absorbing capacity of rBC particles. Understanding the dependence of the increasing rates of F_{rBC} and MAC_{rBC} as a function of OX may lead to improvements of climate models that deal with the warming effects, but more studies in different cities and seasons are needed to gauge the broader implications of these findings.

1. Introduction

Black carbon (BC) aerosol is emitted into the atmosphere mainly through the incomplete combustion of fossil fuels and biomass. These particles efficiently absorb solar radiation, and they have been recognized as the second largest contributor to anthropogenic radiative forcing after carbon dioxide (Jacobson 2001, Ramanathan and Carmichael 2008, Bond *et al* 2013). Estimates of the BC direct radiative forcing have generally ranged from 0.2 to 0.8 W m^{-2} (Jacobson 2001, Kim *et al* 2008, Bond *et al* 2011). Although the importance of BC in the context of global warming has long been recognized, the Fifth Assessment of the Intergovernmental Panel on Climate Change (IPCC) highlighted the fact that there are still large uncertainties in magnitude of the BC direct radiative effects (IPCC 2013).

Variations in the BC direct radiative forcing in different regions can be explained by the differences in the emission, transport, aging, and removal of BC particles (Shiraiwa *et al* 2008, Schwarz *et al* 2010, Bond *et al* 2013). The aging of BC particles as expressed here refers to the transformation of the BC mixing state, namely, the degree to which BC particles become coated with other chemical substances. This is one of

main factors that have led to large discrepancies in model estimates of radiative effects because those results are affected by whether the BC particles are treated as internally- or externally-mixed with other materials. Fresh BC particles from many sources, including fossil fuel combustion, tend to be hydrophobic, and they are initially externally mixed with other particulate matter, but they become internally mixed and more hydrophilic as coatings by other components accumulate during atmospheric aging (McMeeking *et al* 2011a, Liu *et al* 2013). Both physical and chemical processes, including coagulation, condensation, and heterogeneous reactions, can cause changes in the BC mixing state (Kondo *et al* 2011a, Liu *et al* 2013, Browne *et al* 2015).

The BC mixing state plays a crucial role in determining the particles' optical properties because light-scattering materials can refract sunlight to the BC cores through a 'lens effect', and this can amplify the heating potential of BC-containing particles (Lack and Cappa 2010). Both chamber experiments and field observations have shown that the light absorption of BC can be significantly enhanced by internal mixing. For example, Schnaiter *et al* (2005) investigated diesel-soot particles coated with secondary organic compounds, and they found an absorption enhancement of 1.8–2.1 fold for internally-mixed BC compared with externally-mixed BC. Results presented by Liu *et al* (2015) clearly demonstrated that coatings can substantially enhance light absorption by BC emitted from mixed fossil fuel and residential solid fuel combustion sources in the UK during winter. On the other hand, Cappa *et al* (2012) found that the average absorption enhancement was small, only 6%, as BC particles underwent photochemical aging at two sites in California. These discrepancies show that the optical properties of BC particles vary in complex ways with respect to their chemical and physical characteristics, including composition, size, shape, and mixing state.

Photochemical oxidation plays an important role in the evolution of BC mixing state. The term oxidant (OX) as used here is the sum of the ozone and nitrogen dioxide mixing ratios (O_3 + NO_2), and it can be considered as a proxy for atmospheric aging caused by photochemical reactions (Jenkin 2014, Canonaco *et al* 2015). In the urban atmosphere, OX is a more conserved tracer of photochemical processing than O_3 alone because fresh emissions of NO can react with O_3 to form NO_2 (Herndon *et al* 2008). In this paper, we report results from wintertime measurement campaigns in Beijing and Xi'an, China. The mixing state of the refractory black carbon (rBC) particles was determined with a single particle soot photometer (SP2) and light absorption was measured with a photoacoustic extinctiometer (PAX). The mixing ratios of OX, calculated from data obtained with O_3 and NO_x (NO + NO_2) analyzers, were used to represent the atmospheric oxidation capacity. The objective of the study was to investigate how two important properties of the rBC, that is, the mixing state and mass absorption cross-section, were related to the atmospheric oxidation capacity in the urban atmosphere of China.

2. Experimental methods

The studies were conducted at two urban sites, one in Beijing and the second in Xi'an, China (see supplemental figure S1 available at stacks.iop.org/ERL/12/044012/mmedia). Beijing is one of the largest cities in the world (population > 21 million), and it is located in an area bordering the North China Plain and the Inner Mongolia Plateau; it is surrounded by the Yanshan Mountains to the north and Taihang Mountains to the west. The measurements in Beijing were made on the rooftop of the Institute of Remote Sensing Applications (IRSA, ~18 m above ground level, 40.01°N, 116.39°E, Wang *et al* 2016a) from 1 to 18 February 2014. The sampling site is surrounded by an educational district and the Olympic Park; to the south is the Datun Road (~450 m), where the traffic is heavy, while to the east is the Beichen West Road (~150 m), which has less traffic. Xi'an is located on the Guanzhong Plain at the southern edge of the Loess Plateau, and it is the largest city in Northwest China (population of >8 million). The measurements in Xi'an were made on the rooftop of the Institute of Earth Environment, Chinese Academy of Sciences (IEECAS, ~10 m above ground level, 34.23°N, 108.88°E, Cao *et al* 2009) from 8 to 20 February 2013. The Xi'an sampling site is surrounded by residential/commercial areas, and no major industrial sources are located nearby. To the east is the Fenghui South Road (~20 m), where the traffic is usually light. Both sampling sites are located in urban zones, and they may be considered generally representative of urban conditions. Due to the rapid economic development, population growth, and urbanization over the past decades, both cities often suffer from high loadings of particulate pollutants (Cao *et al* 2012, Huang *et al* 2014). Previous studies had shown that coal burning is the most important source for rBC during the winter in Beijing (Schleicher *et al* 2013) while traffic is the dominant wintertime source for rBC in Xi'an (Wang *et al* 2016b).

The mixing state of individual rBC particles was determined with a commercially available SP2 instrument (Droplet Measurement Technologies, Boulder, CO, USA). The operating principles of the SP2 have been described in detail elsewhere (Schwarz *et al* 2006, Gao *et al* 2007, Cross *et al* 2010). Briefly, the SP2 uses a continuous intra-cavity Nd:YAG laser (1064 nm) with a Gaussian profile (TEM00 mode) to heat rBC-containing particles to their vaporization point, which causes the emission of an incandescence signal. The peak intensity of the incandescence signal

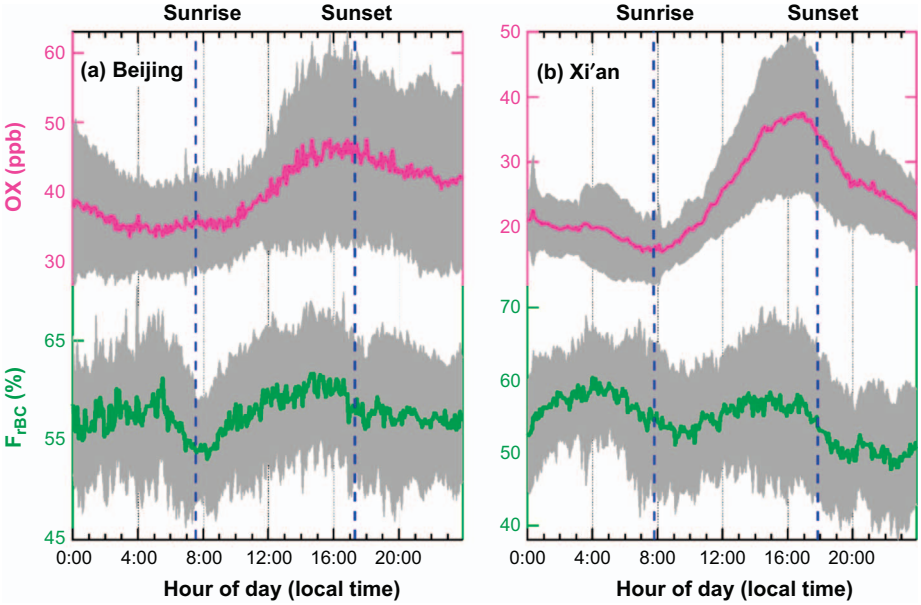

Figure 1. Diurnal variations of 5 min average number fraction of thickly coated refractory black carbon (F_{rBC}) and oxidant (OX) mixing ratios at (*a*) Beijing and (*b*) Xi'an for all samples. The grey shaded regions represent the averages ± one standard deviation.

is linearly related to the rBC mass, and it is influenced little by the particles' mixing state or morphology (Slowik *et al* 2007, Kondo *et al* 2011b). The time delay between the occurrence of the scattering and incandescence signal peaks is used to determine whether individual rBC particles are internally-mixed with non-rBC materials (Schwarz *et al* 2006, McMeeking *et al* 2011b, Perring *et al* 2011). Time delays occur because the coatings must be removed from the rBC particles before the onset of incandescence. In this study, time delays of ~3 μs and ~2 μs were used as the criteria for distinguishing thickly-coated rBC particles from uncoated or thinly-coated ones at Beijing and Xi'an, respectively. These criteria were based on the minima in the bimodal frequency distributions of the time delays for the full study periods at the two sites (see below figure 2). The incandescence signal was calibrated using standard fullerene soot samples (Lot F12S011, Alpha Aesar, Inc., Ward Hill, Massachusetts). The uncertainty in the rBC mass determination was estimated to be ~25%. More details concerning the IEECAS SP2 operation and calibration can be found in our previous publication (Wang *et al* 2014).

The particulate light absorption coefficient at λ = 532 nm was measured using a PAX (Droplet Measurement Technologies, Boulder, CO, USA). The PAX uses intracavity photoacoustic technology to directly measure the light absorption of aerosol particles. A laser beam produced by a modulated diode in the acoustic chamber of the instrument heats suspended absorbing aerosol particles, and the resulting pressure wave is detected with a sensitive microphone. Different mixing ratios of NO_2 were used to calibrate the instrument before and after the experiments.

Mixing ratios of O_3 and NO_2, measured as 5 min averages, were obtained using a Model EC9810 photometric ozone analyzer (Ecotech Pty Ltd, Knoxfield, Australia) and a Model EC9841 NO/NO_2/NO_x (Ecotech Pty Ltd, Knoxfield, Australia) gas-phase chemiluminescence instrument, respectively. Standard reference O_3 and NO gases were used to calibrate the ozone and nitrogen oxides analyzers before and after the experiments. Relative humidity (RH) and temperature (5 min averages) were measured using an automatic weather station (MAWS201, Vaisala, Vantaa, Finland) configured with an RH/temperature probe (Model QMH101). The absolute humidity was estimated using the RH and temperature data.

3. Results and discussion

3.1. Characterization of OX

Significant variations in the time-resolved (5 min averages) in OX were observed over the entire campaign periods at both Beijing and Xi'an, with mixing ratios ranging from 19 to 79 ppb and 10 to 60 ppb and averaging 40 ± 11 ppb and 25 ± 10 ppb at the two sites, respectively (supplemental figure S2). Differences in the daily levels of O_3 precursor gases (NO_x) and volatile organic compounds (VOCs) as well as the O_3-NO_x-VOCs coupled chemistry presumably were the main factors influencing the variations in the day-to-day OX values (Tang *et al* 2012, Feng *et al* 2016). Although O_3 contributed only ~30% to the OX at both sites on average, the O_3/OX ratios increased to ~50% in the afternoon when OX reached its daily maximum.

A plot of the 5 min average OX mixing ratios (figure 1) shows that OX exhibited similar diurnal

patterns at Beijing and Xi'an. The daily minimum occurred at ~08:00 loca time (LT, all time references that follow are given in LT) followed by a sharp increase to a daytime peak in the afternoon at ~16:00. Then, the OX mixing ratios declined continuously until the early morning of the following day. This diurnal cycle is typical of what has been found in other urban areas (Notario *et al* 2012), and it is likely driven by variations in local anthropogenic activities, photochemical conditions, and atmospheric boundary layer heights. The low OX values early in the day can be attributed to heavy motor vehicle emissions from the morning rush hour. It can be seen in Supplemental figure S3 that the NO mixing ratios at both sites reached high values at ~08:00, which is when low O_3 values were observed, mostly likely due to the titration of O_3 by NO (Shaw *et al* 2015, Wang *et al* 2015). Increase in OX after sunrise were probably due to the photochemical production of O_3 and to some extent vertical mixing. Low mixing ratios of OX during the night can be explained by the lack of photochemical production and losses through titration reactions and surface deposition (Wang *et al* 2012).

3.2. Effect of photochemical oxidation on rBC mixing state

The number fraction of thickly-coated rBC (F_{rBC}) is a good indicator of the percentage of rBC particles internally mixed with other substances, and it is calculated as the ratio between the number of thickly-coated rBC particles and total number of measured rBC particles. The mixing state of rBC can vary for particles from different sources; for example, rBC particles from biomass burning are more likely to be coated than those from traffic emissions (Schwarz *et al* 2008, Liu *et al* 2014). In addition, F_{rBC} typically is higher for more aged rBC particles than fresh ones because coatings can accumulate through various atmospheric processes over time (McMeeking *et al* 2011b, Huang *et al* 2012). As we sampled rBC particles from a complex mixture of sources, the daily variations in F_{rBC} were likely due to changes in the relative contributions of various rBC sources as well as subsequent aging of the particles. Supplemental figure S2 shows that F_{rBC} ranged from 35% to 92% with arithmetic mean of 59 ± 7% at Beijing and varied from 27% to 76% with average of 55 ± 9% at Xi'an. In comparison with previous studies made with SP2s deployed in other Chinese areas, the F_{rBC} values at Beijing and Xi'an were comparable to those in winter at Jiaxing (Huang *et al* 2013) and autumn at Qinghai Lake (Wang *et al* 2014) where the averages were 53% and 50%, respectively. However, the F_{rBC} at Beijing and Xi'an were higher than what was reported for spring/summer in Shanghai (Huang *et al* 2012) and spring in Xiamen (Wang *et al* 2016c) where the average values were 41% and 31%, respectively. These differences simply show that there are substantial spatial and temporal variability in the rBC mixing state in China.

Figure 1 shows that F_{rBC} exhibited similar diurnal patterns at Beijing and Xi'an with 'two peaks and two valleys' each day. The lower valley in the early morning around 07:00–09:00 can be explained by increases in fresh rBC particles emitted by local rush-hour traffic. At both sites, F_{rBC} increased after sunrise and peaked at 15:00–16:00, and that was followed by a continuous decrease until sunset. The diurnal pattern of F_{rBC} is broadly consistent with the variations of OX, indicating that photochemical oxidation may play an important role in the evolution of the rBC mixing state. The F_{rBC} showed comparable rates of increase from 08:00 to 16:00 at the two sites, 0.8 % h^{-1} ($r = 0.96$) at Beijing and 0.6 % h^{-1} ($r = 0.80$) at Xi'an. Low F_{rBC} values during the night (19:00–23:00) may be explained by the production of particles from primary anthropogenic emissions, especially those from heating activities at night. As the night progressed, the emitted rBC particles aged in the relatively shallow boundary layer and that led to another peak of F_{rBC} at 03:00–05:00. However, identifying the specific mechanisms involved in the rBC night-time aging process is beyond the scope of this study, and further research is needed to uncover the mechanisms and processes responsible for this internal mixing.

To investigate possible effects of photochemistry on the rBC mixing state, the data collected from 08:00 to 16:00—a period when OX typically increased—were examined to determine how the fraction of thickly-coated rBC changed with OX. Seventeen out of eighteen sampling days at Beijing and eleven out of thirteen sampling days at Xi'an showed increasing trends in OX from 08:00–16:00 (see vertical yellow and grey shading in Supplemental figure S2) while the remaining days at both sites exhibited decreasing OX trends (see light cyan shades). The F_{rBC} values broadly tracked increases in OX except for the samples from 2, 8, and 16 February at Beijing and 12 and 17 February at Xi'an (see vertical grey shades in figure S2). Those five days were characterized by large variations in meteorological conditions; for example, as shown in figure S2, the absolute humidity between 08:00 and 16:00 sharply decreased on those five days but was rather constant on the other days. These changes in absolute humidity suggest the advection of air masses with different histories and characteristics than what was sampled during the more common conditions. More specifically, the lower humidity indicates either intrusions of free tropospheric air or advection of air from much drier areas, and neither of those cases would be optimal for studying the effects of the local/regional chemistry. Thus, the data for those five days as well as the three days on which OX decreased were excluded in the following analysis and discussion.

The distributions of the time delays (Δt) between the scattering and incandescence signal peaks were used to investigate potential impact of photochemistry

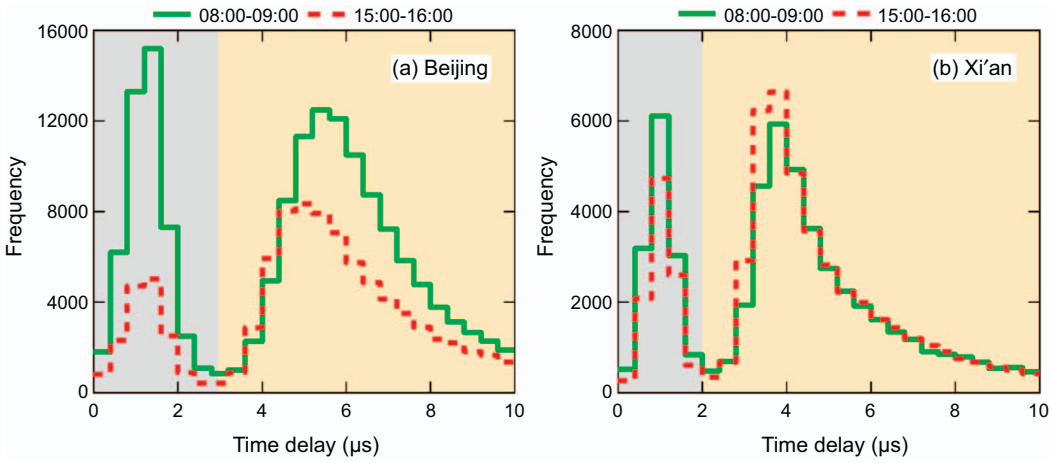

Figure 2. Frequency distributions of the time delays between the scattering and incandescence signal peaks of the SP2 for rBC particles sampled at 08:00–09:00 and 15:00–16:00 local time at (*a*) Beijing and (*b*) Xi'an during the entire campaign. The grey and yellow regions represent the uncoated or thinly-coated rBC particles and the thickly-coated ones, respectively.

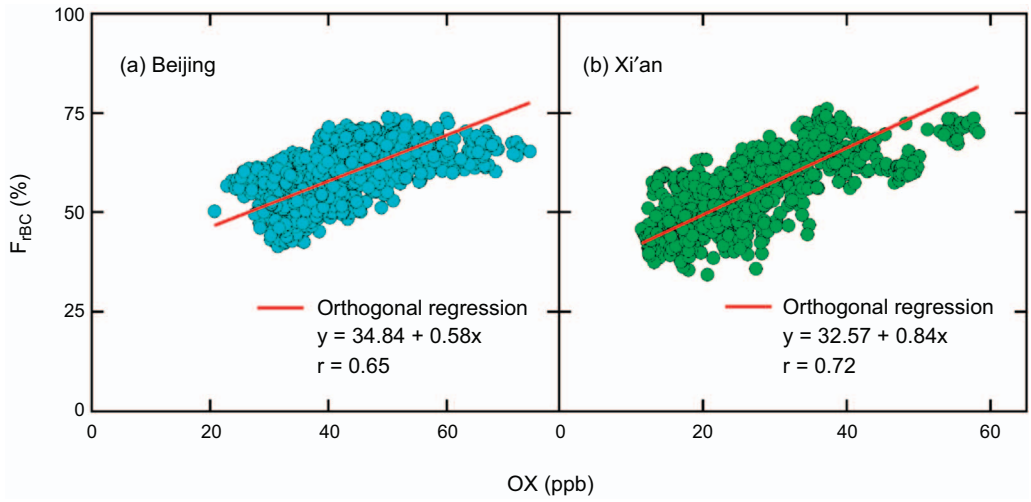

Figure 3. Correlations between number fraction of thickly-coated rBC (F_{rBC}) and oxidant (OX) mixing ratios at (*a*) Beijing and (*b*) Xi'an at 08:00–16:00 local time.

on the rBC mixing state. Figure 2 shows the frequency distributions of Δt at Beijing and Xi'an for rBC-containing particles measured at 08:00–09:00 (lowest OX level) and at 15:00–16:00 (highest OX level) for the entire campaign periods. The frequency distributions for Δt from both sites were bimodal: one peak occurred at a time delay of ~1.2 μs for Beijing and ~0.8 μs for Xi'an (short-Δt) and the other at ~5.0 μs for Beijing and ~3.5 μs for Xi'an (long-Δt); these two peaks represent the thinly- and thickly-coated rBC particles, respectively (see Methods). From 08:00–09:00, a large fraction of the particles clustered at the short-Δt, reflecting the important contribution of thinly-coated rBC to the total rBC population; at 15:00–16:00, when photochemical oxidation processes were more active, a larger fraction of the particles clustered at the long-Δt, indicating that more of the rBC particles were thickly-coated.

To further investigate the impact of oxidant levels on the rBC mixing state, the F_{rBC} data collected between 08:00–16:00 at both sites are plotted against OX mixing ratios in figure 3. It can be seen that F_{rBC} was positively correlated with OX ($r = 0.65$ for Beijing and 0.72 for Xi'an), indicating greater fractions of coated rBC particles under more oxidizing conditions. The enhancement in thickly-coated rBC observed between 08:00–16:00 can be explained by the photochemical production of secondary substances, including both inorganic and organic non-refractory compounds, which condensed onto the rBC. The slopes of the F_{rBC} versus OX were 0.58% ppb^{-1} for Beijing and 0.84% ppb^{-1} for Xi'an, respectively, which may reflect differences in the oxidation rates of the rBC particles at the two sites. That is, a stronger effect at Xi'an compared with Beijing can be attributed to the more rapid increase in OX at Xi'an (2.9 ppb h^{-1}) compared to Beijing (1.8 ppb h^{-1}).

3.3. Effect of photochemical oxidation on MAC_{rBC}

The mass absorption cross-section of rBC (MAC_{rBC}, in m^2 g^{-1}) is one of the most informative optical

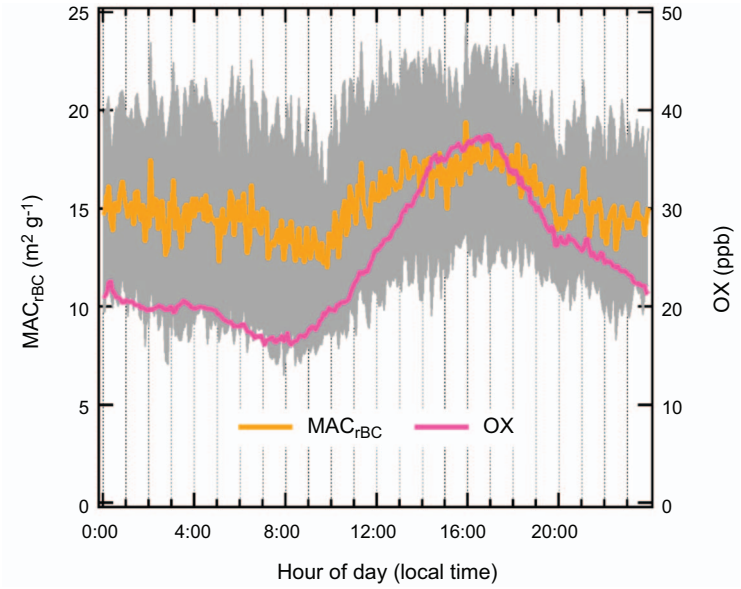

Figure 4. Diurnal variations of 5 min averaged rBC mass absorption cross-sections (MAC_{rBC}) and oxidant (OX) mixing ratios at Xi'an. The grey shaded region represents the averages ± one standard deviation for the MAC_{rBC} values.

properties of the rBC aerosol because it reflects the relationship between the radiative effects of the rBC particles and their mass. The MAC_{rBC} is calculated by dividing the absorption coefficient (σ_{abs}) measured with the PAX by the rBC mass concentration from the SP2 ($MAC_{rBC} = \sigma_{abs}/[rBC]$). It is worth noting that the MAC_{rBC} calculated in this way should be considered as an upper limit because even though their contributions are usually small, other chemical species, such as brown carbon, also can contribute to light absorption in mid-visible wavelengths (Laskin *et al* 2015). Due to the lack of PAX measurements in Beijing, the MAC_{rBC} values could only be calculated for Xi'an, and those results are discussed below.

The MAC_{rBC} values generally followed a Gaussian distribution and showed a peak at 12.7 $m^2 g^{-1}$ (supplemental figure S4). The overall average for the campaign was 14.6 ± 5.6 $m^2 g^{-1}$, which is ~1.9 times higher than the value of 7.8 $m^2 g^{-1}$ (extrapolated to 532 nm from 550 nm, assuming an absorption Ångström exponent of 1.0) that was suggested to be generally representative of uncoated rBC particles (Bond and Bergstrom 2006). The relatively high MAC_{rBC} at Xi'an suggests that absorption was affected by internal mixing with other materials. Indeed, the internal mixing of rBC does increase the absorption of visible light, partly because the non-absorbing materials act like a lens and therefore refract light toward the absorbing rBC core (Lack and Cappa 2010).

Figure 4 shows that a daily minimum in the 5 min average MAC_{rBC} values occurred ~08:00–09:00; the MAC_{rBC} then started to increase at a rate of 0.6 $m^2 g^{-1} h^{-1}$ until attaining the maximum value at 16:00. As day turned to night, the MAC_{rBC} decreased at a rate of 0.2 $m^2 g^{-1} h^{-1}$ until early morning. This diurnal pattern in MAC_{rBC} was similar to the variations seen in the OX mixing ratios measured in parallel, and this suggests that the enhancement of the MAC_{rBC} was largely driven by photochemical processes. We plotted the MAC_{rBC} values against the OX mixing ratios between 08:00 and 16:00 for the days when OX was increasing (figure 5) to focus on the interval of increasing OX. This plot shows that MAC_{rBC} was positively correlated ($r = 0.71$) with the OX mixing ratios, and these results further support the argument that photochemical processes led to increases in MAC_{rBC}. It can also be seen in figure 5 that MAC_{rBC} increased with increasing F_{rBC} values, and although the relationship was not strong, it was statistically significant ($r = 0.60$, $p < 0.05$).

Positive correlations among MAC_{rBC}, F_{rBC}, and OX indicate that more oxidizing conditions favor the formation of secondary aerosol coatings on the rBC particles, which in turn enhance the particles' absorption efficiencies. The slope of 0.26 $m^2 g^{-1}$ ppb^{-1} obtained from an orthogonal regression is arguably representative of the rate at which photochemical oxidation altered the MAC_{rBC}. Results of a study by Cappa *et al* (2012) showed that the absorption enhancement increased more weakly with photochemical aging in California compared with our results. This implies that megacities in North America, and likely other parts of the world, may need to be treated differently compared with those in Asia where the concentrations particulate and secondary components are typically quit high (Huang *et al* 2014). Indeed, additional studies in different areas and other seasons are needed for more reliable and comprehensive assessments of the effects of oxidants on the optical properties and environmental effects—especially the warming potential—of rBC particles.

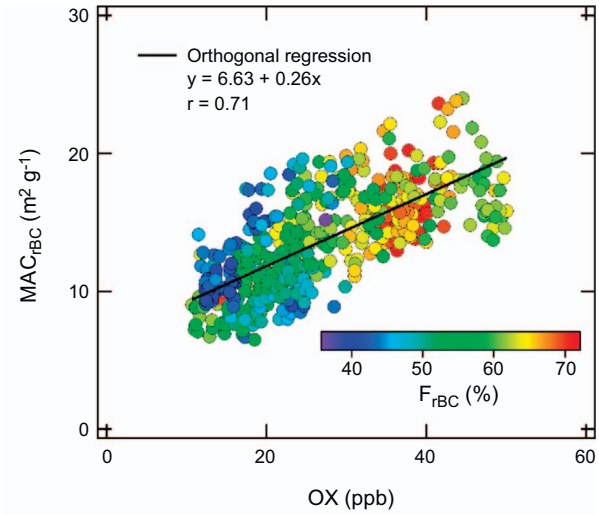

Figure 5. Correlation between the mass absorption cross-section of refractory black carbon (MAC_{rBC}) and oxidant (OX) mixing ratios. Data points are color-coded with respect to the number fraction of thickly coated rBC (F_{rBC}).

4. Conclusions

The mixing state of refractory black carbon (rBC) was measured with a single particle soot photometer (SP2) at Xi'an and Beijing, China, in February 2013 and 2014, respectively. The number fraction of thickly-coated rBC particles (F_{rBC}), expressed as a percentage, was used to determine the degree to which the rBC particles were internally mixed with other materials. The overall average F_{rBC} values for the campaigns were 59 ± 7% at Beijing and 55 ± 9% at Xi'an, and the percentages of internally-mixed particles increased after sunrise. On average, from 08:00 to 16:00, F_{rBC} increased at a rate of 0.8% h^{-1} at Beijing and 0.6 % h^{-1} at Xi'an, and these enhancements in the percentages of coated rBC particles were paralleled by increases in oxidant ($OX = O_3 + NO_2$) mixing ratios. Strong correlations between F_{rBC} and OX were found between 08:00 and 16:00 at both sites, suggesting that the photochemical oxidation plays an important role in forming the rBC coatings. Regression analyses showed that the rate of increase in F_{rBC} with OX was greater at Xi'an than Beijing (0.84 versus 0.58% ppb^{-1}), suggesting that the rBC particles in Xi'an were more rapidly coated that those in Beijing.

Light absorption measurements were not made at Beijing, but similar to F_{rBC}, the mass absorption cross-section of rBC (MAC_{rBC}) at Xi'an tracked the increases in OX. Indeed, the MAC_{rBC} varied linearly with the OX mixing ratios, and therefore the coatings on the rBC that resulted from photochemical reactions evidently increased the particles' absorption efficiencies. The slope of $+0.26\,m^2\,g^{-1}$ ppb^{-1} for the orthogonal regression between MAC_{rBC} and OX is a measure of the rate at which the MAC_{rBC} increased at Xi'an during the daytime. The mixing state and optical properties of rBC particles are among the most critical parameters used in the global and regional models of radiative forcing. Photochemically-induced changes in F_{rBC} and MAC_{rBC} should be investigated for different areas and seasons, and the results of those studies should be included in climate models to provide more reliable assessments of the warming potential of rBC particles.

Acknowledgments

This work was supported by the 'Strategic Priority Research Program' of the Chinese Academy of Sciences (XDB05060500, XDA05100400), the National Natural Science Foundation of China (No. 41230641, 41503118, and 41403110), and the China Postdoctoral Science Foundation (2015M580890).

References

Bond T C and Bergstrom R W 2006 Light absorption by carbonaceous particles: an investigative review *Aerosol Sci. Technol.* **40** 27–67

Bond T C, Zarzycki C, Flanner M G and Koch D M 2011 Quantifying immediate radiative forcing by black carbon and organic matter with the specific forcing pulse *Atmos. Chem. Phys.* **11** 1505–25

Bond T C *et al* 2013 Bounding the role of black carbon in the climate system: a scientific assessment *J. Geophys. Res.* **118** 5380–552

Browne E C, Franklin J P, Canagaratna M R, Massoli P, Kirchstetter T W, Worsnop D R, Wilson K R and Kroll J H 2015 Changes to the chemical composition of soot from heterogeneous oxidation reactions *J. Phys. Chem.* A **119** 1154–63

Canonaco F, Slowik J G, Baltensperger U and Prévôt A S H 2015 Seasonal differences in oxygenated organic aerosol composition: implications for emissions sources and factor analysis *Atmos. Chem. Phys.* **15** 6993–7002

Cao J-J, Zhu C-S, Chow J C, Watson J G, Han Y-M, Wang G-H, Shen Z-X and An Z-S 2009 Black carbon relationships with emissions and meteorology in Xi'an, China *Atmos. Res.* **94** 194–202

Cao J J, Wang Q Y, Chow J C, Watson J G, Tie X X, Shen Z X, Wang P and An Z S 2012 Impacts of aerosol compositions on visibility impairment in Xi'an, China *Atmos. Environ.* **59** 559–66

Cappa C D *et al* 2012 Radiative absorption enhancements due to the mixing state of atmospheric black carbon *Science* **337** 1078–81

Cross E S *et al* 2010 Soot particle studies—instrument inter-comparison—project overview *Aerosol Sci. Technol.* **44** 592–611

Feng T *et al* 2016 Summertime ozone formation in Xi'an and surrounding areas, China *Atmos. Chem. Phys.* **16** 4323–42

Gao R S *et al* 2007 A novel method for estimating light-scattering properties of soot aerosols using a modified single-particle soot photometer *Aerosol Sci. Technol.* **41** 125–35

Herndon S C *et al* 2008 Correlation of secondary organic aerosol with odd oxygen in Mexico City *Geophys. Res. Lett.* **35** L15804

Huang R-J *et al* 2014 High secondary aerosol contribution to particulate pollution during haze events in China *Nature* **514** 218–22

Huang X-F, He L-Y, Xue L, Sun T-L, Zeng L-W, Gong Z-H, Hu M and Zhu T 2012 Highly time-resolved chemical characterization of atmospheric fine particles during 2010 Shanghai World Expo *Atmos. Chem. Phys.* **12** 4897–907

Huang X-F, Xue L, Tian X-D, Shao W-W, Sun T-L, Gong Z-H, Ju W-W, Jiang B, Hu M and He L-Y 2013 Highly time-resolved carbonaceous aerosol characterization in Yangtze River Delta of China: composition, mixing state and secondary formation *Atmos. Environ.* **64** 200–7

IPCC 2013 Climate change 2013: the physical science basis *Contribution of Working Group I to the Fifth Assessment Report of the Intergovernmental Panel on Climate Change* ed T F Stocker *et al* (Cambridge UK: Cambridge University Press)

Jacobson M Z 2001 Strong radiative heating due to the mixing state of black carbon in atmospheric aerosols *Nature* **409** 695–7

Jenkin M E 2014 Investigation of an oxidant-based methodology for AOT40 exposure assessment in the UK *Atmos. Environ.* **94** 332–40

Kim D, Wang C, Ekman A M, Barth M C and Rasch P J 2008 Distribution and direct radiative forcing of carbonaceous and sulfate aerosols in an interactive size-resolving aerosol-limate model *J. Geophys. Res.* **113** D16309

Kondo Y *et al* 2011a Emissions of black carbon, organic, and inorganic aerosols from biomass burning in North America and Asia in 2008 *J. Geophys. Res.* **116** D08204

Kondo Y, Sahu L, Moteki N, Khan F, Takegawa N, Liu X, Koike M and Miyakawa Y 2011b Consistency and traceability of black carbon measurements made by laser-induced incandescence, thermal-opitcal transmittance, and filter-based photo-absorption techniques *Aerosol Sci. Technol.* **45** 295–312

Lack D and Cappa C 2010 Impact of brown and clear carbon on light absorption enhancement, single scatter albedo and absorption wavelength dependence of black carbon *Atmos. Chem. Phys.* **10** 4207–20

Laskin A, Laskin J and Nizkorodov S A 2015 Chemistry of atmospheric brown carbon *Chem. Rev.* **115** 4335–82

Liu D, Allan J, Whitehead J, Young D, Flynn M, Coe H, McFiggans G, Fleming Z and Bandy B 2013 Ambient black carbon particle hygroscopic properties controlled by mixing state and composition *Atmos. Chem. Phys.* **13** 2015–29

Liu D *et al* 2014 Size distribution, mixing state and source apportionment of black carbon aerosol in London during wintertime *Atmos. Chem. Phys.* **14** 10061–84

Liu S *et al* 2015 Enhanced light absorption by mixed source black and brown carbon particles in UK winter *Nat. Commun.* **6** 8435

McMeeking G R, Good N, Petters M D, McFiggans G and Coe H 2011a Influences on the fraction of hydrophobic and hydrophilic black carbon in the atmosphere *Atmos. Chem. Phys.* **11** 5099–112

McMeeking G, Morgan W, Flynn M, Highwood E, Turnbull K, Haywood J and Coe H 2011b Black carbon aerosol mixing state, organic aerosols and aerosol optical properties over the United Kingdom *Atmos. Chem. Phys.* **11** 9037–52

Notario A, Bravo I, Adame J A, Díaz-de-Mera Y, Aranda A, Rodríguez A and Rodríguez D 2012 Analysis of NO, NO_2, NO_x, O_3 and oxidant ($OX = O_3 + NO_2$) levels measured in a metropolitan area in the southwest of Iberian Peninsula *Atmos. Res.* **104** 217–26

Perring A E *et al* 2011 Characteristics of black carbon aerosol from a surface oil burn during the deepwater horizon oil spill *Geophys. Res. Lett.* **38** L17809

Ramanathan V and Carmichael G 2008 Global and regional climate changes due to black carbon *Nat. Geosci.* **1** 221–7

Schleicher N, Norra S, Fricker M, Kaminski U, Chen Y, Chai F, Wang S, Yu Y and Cen K 2013 Spatio-temporal variations of black carbon concentrations in the Megacity Beijing *Environ. Pollut.* **182** 392–401

Schnaiter M, Linke C, Möhler O, Naumann K H, Saathoff H, Wagner R, Schurath U and Wehner B 2005 Absorption amplification of black carbon internally mixed with secondary organic aerosol *J. Geophys. Res.* **110** D19204

Schwarz J P *et al* 2006 Single-particle measurements of midlatitude black carbon and light-scattering aerosols from the boundary layer to the lower stratosphere *J. Geophys. Res.* **111** D16207

Schwarz J P *et al* 2008 Measurement of the mixing state, mass, and optical size of individual black carbon particles in urban and biomass burning emissions *Geophys. Res. Lett.* **35** L13810

Schwarz J P, Spackman J R, Gao R S, Watts L A, Stier P, Schulz M, Davis S M, Wofsy S C and Fahey D W 2010 Global-scale black carbon profiles observed in the remote atmosphere and compared to models *Geophys. Res. Lett.* **37** L18812

Shaw M D, Lee J D, Davison B, Vaughan A, Purvis R M, Harvey A, Lewis A C and Hewitt C N 2015 Airborne determination of the temporo-spatial distribution of benzene, toluene, nitrogen oxides and ozone in the boundary layer across Greater London, UK *Atmos. Chem. Phys.* **15** 5083–97

Shiraiwa M, Kondo Y, Moteki N, Takegawa N, Sahu L K, Takami A, Hatakeyama S, Yonemura S and Blake D R 2008 Radiative impact of mixing state of black carbon aerosol in Asian outflow *J. Geophys. Res.* **113** D24210

Slowik J G *et al* 2007 An inter-comparison of instruments measuring black carbon content of soot particles *Aerosol Sci. Technol.* **41** 295–314

Tang G, Wang Y, Li X, Ji D, Hsu S and Gao X 2012 Spatial-temporal variations in surface ozone in Northern China as observed during 2009–2010 and possible implications for future air quality control strategies *Atmos. Chem. Phys.* **12** 2757–76

Wang Q, Schwarz J P, Cao J, Gao R, Fahey D W, Hu T, Huang R-J, Han Y and Shen Z 2014 Black carbon aerosol characterization in a remote area of Qinghai–Tibetan Plateau, western China *Sci. Total Environ.* **479** 151–8

Wang Q Y, Gao R S, Cao J J, Schwarz J P, Fahey D W, Shen Z X, Hu T F, Wang P, Xu X B and Huang R-J 2015 Observations of high level of ozone at Qinghai Lake basin in the northeastern Qinghai-Tibetan plateau, western China *J. Atmos. Chem.* **72** 19–26

Wang Q *et al* 2016a Contribution of regional transport to the black carbon aerosol during winter haze period in Beijing *Atmos. Environ.* **132** 11–8

Wang Q *et al* 2016b Physicochemical characteristics of black carbon aerosol and its radiative impact in a polluted urban area of China *J. Geophys. Res. Atmos.* **121** 12505–19

Wang Q *et al* 2016c Size distribution and mixing state of refractory black carbon aerosol from a coastal city in South China *Atmos. Res.* **181** 163–71

Wang X, Shen Z, Cao J, Zhang L, Liu L, Li J, Liu S and Sun Y 2012 Characteristics of surface ozone at an urban site of Xi'an in Northwest China *J. Environ. Monit.* **14** 116–26